Shuang Huang*
Xin Wu
Peixing Li

Influence of Temperature on the Properties of Cellulose Iβ based on Molecular Dynamics Simulations

DOI: 10.5604/01.3001.0015.2719

Shanghai University of Engineering Science,
College of Mechanical
and Automotive Engineering,
No 333 Longteng Road, Songjiang,
Shanghai 201620, China,
* e-mails: huangshuang1989@126.com

Abstract
Natural plants, such as cotton and linen, are rich in cellulose Iβ. The properties of cellulose Iβ under different temperatures was studied using molecular dynamics simulations. Firstly, the crystal of cellulose Iβ was built. To verify the model, the X-ray fibre diffraction and thermal expansion coefficients were calculated, which were found to agree with experimental results. Then the Mulliken population of the bonds were computed and the movement of the centre chain and hydrogen bonds studied over the range 300-550 K using a PCFF force field. The results of the Mulliken population reveal the three steps of pyrolysis. The higher the temperature is, the more intensely the movement of the centre chain is. However, the impact of temperature on the movement of the centre chain is not obvious. From 300 K to 550 K, the total number of hydrogen bonds decreased by only 20%. Moreocer, the rupture of intrachain hydrogen bonds and the formation of interchain hydrogen bonds at 400 K~450 K temperature occurred.

Key words: *cellulose Iβ; molecular dynamics simulations; Mulliken population; movement of chain; hydrogen bonds.*

Introduction

With the rapid development of the global economy and general increase in the level of consumption, there is a growing preference for natural fibres with excellent wear abilities. To improve the performance of natural fibres, firstly their structure fibre should be understood. High crystallinity of cellulose is found in most natural textile fibres, especially cotton and hemp fibre. The structure of cellulose is a linear homopolymer of β (1-4)-linked D-glucose units, and the disaccharide repeat unit of this polymer is cellobiose. Nowadays, cellulose has four principal polymorphs: I, II, III and IV [1]. Native cellulose consists of two allomorphs, which are labeled Iα and Iβ. Under certain conditions, the Iα phase can be converted to an Iβ phase in a solid state [2]. Electron diffraction analysis reveals that the Iβ phase corresponds to a two-chain monoclinic unit cell and the Iα phase to a one-chain triclinic unit cell [3-5]. And the cellulose of ramie and cotton is dominated by Iβ, whereas bacterial and Valonia celluloses are rich in Iα. Thus, in this paper, cellulose Iβ was taken as the research object.

Recently, some scholars have done some researches on cellulose properties. Cellulose Iβ undergoes a transition into a high-temperature phase with the temperature increasing above 220 ~ 230 °C, which is investigated with X-ray diffraction [6, 7]; this result is also proved by using the infrared spectrum [8, 9]. The Young's modulus of cellulose Iβ is calculated using molecular dynamics simulations, which agrees with the experimental value at room temperature [10]; the density, thermal expansion coefficients, total dipole moment, and the static dielectric constant are computed under a GROMOS 45a4 force field [11]. While the properties of cellulose Iβ at room temperature and experimental protocol for structural transformation are well established, atomistic details of the structural changes under different temperatures are still unknown.

The temperature in a modification kettle device was measured in real time in the temperature range from 300 K to 550 K. Thus, the diffusion behaviour of the ammonia molecule from 300 K to 550 K was studied. In this paper, all simulations were implemented using Materials Studio 5.5 under a PCFF (polymer consistent force field) force field developed on the basis of a CFF91 force field [12-13]. The focus was on the study of polymer and polymer materials, such as polycarbonate, polysaccharide and carbohydrate. The PCFF force field was proven to be very suitable for calculating organic compounds, especially natural polymer materials. The Mulliken population was computed using the CASTEP module. To explain the mechanism of the properties of cellulose Iβ at a molecular level, hydrogen bonds and the movement of the centre chain were studied over the range 300-550 K.

Methods

Model

Modelling is the foundation of understanding the structure and performance of cellulose Iβ. Cellulose Iβ has a two-chain monoclinic unit cell (a = 7.784 Å, b = 8.201 Å, c = 10.38 Å;) with a space group of P21 [14]. The simulation box used in this paper consisted of a 3 × 3 × 3 supercell of cellulose Iβ. A total of 150 glucose units were arranged in 25 chains of a length of 6 glucose units. The detailed structures of cellulose Iβ and the supercell are shown in ***Figure 1***, where the grey atom is C, the red atom O, and the white atom H.

Model verification by X-ray diffraction

To verify the correctness of the cellulose Iβ model, the X-ray diffraction computed (XRD) and the experimental XRD were tested. The XRD computed was completed in a reflex/powder diffraction module, where the crystallite size of cellulose Iβ was set to 50 Å × 50 Å × 50 Å. In the process of the experiment, X-ray diffraction measurements were carried out on a RIGAKU D/max-2550PCX X-ray diffractometer. The test conditions of the simulation and experiment were the same: intensity measurements were performed in the range $5° \leq 2\theta \leq 60$ with Cu $K\alpha$ radiation (λ = 1.540562 Å) generated at 200 mA and 40 KV; the step-scan technique was used with a 0.02° interval at 2θ, with a scanning rate of 5°/min; the $K_{\alpha 2}$ component was removed, and the integral

Huang S, Wu X, Li P. Influence of Temperature on the Properties of Cellulose Iβ based on Molecular Dynamics Simulations.
FIBRES & TEXTILES in Eastern Europe 2021; 29, 6(150): 32-36. **DOI:** 10.5604/01.3001.0015.2719

breadth and full-width at the half-maximum (FWHM) were measured using the software configured with the XRD system.

Crystalline indices of cellulose Iβ samples were calculated from the X-ray diffraction data by ***Equation 1*** [15]:

$$X_C = \frac{I_{002} - I_{am}}{I_{002}} \times 100\% \qquad (1)$$

Where I_{002} is the peak intensity of (0 0 2) the lattice plane (2θ = 22.6°) and I_{am} the peak intensity of amorphous phases (2θ = 18°).

The apparent crystallite size (ACS) was estimated using the Scherrer ***Equation (2)*** [16]:

$$ACS = \frac{0.9\gamma}{\beta \cos\theta} \qquad (2)$$

Where λ is the wavelength of the X-ray (λ = 1.540562 Å), θ the Bragg angle corresponding to the (0 0 2) plane, and β is the half-height width of the peak angle of the (0 0 2) plane.

The simulated XRD and experimental XRD are shown in ***Figure 2***, which match well with each other. This demonstrates that the model of cellulose Iβ is correct. And the results of the crystallinity index and ACS are shown in ***Table 1***. The main cause of small differences between the simulated and experimental results is that the materials of the experiment contain hemicellulose and pectin, whereas the simulation materials ignore these substances.

Model verification by the thermal expansion coefficient

To verify the correctness of the force field and the model, the thermal expansion coefficients of cellulose Ib at different temperatures were calculated, respectively. The changes in lattice parameters *a* and *b* were calculated by using the Forcite/Dynamic module of MS software in the range of 300 K ~ 500 K. The simulation was completed under the NPT ensemble with a pressure of 0.0001 GPa, simulation time of 500 ps, and step length of 1 fs.

The formula for calculating the thermal expansion coefficient is as follows:

$$\alpha = \frac{1}{l_{T=273K}} \frac{dl}{dT} \qquad (3)$$

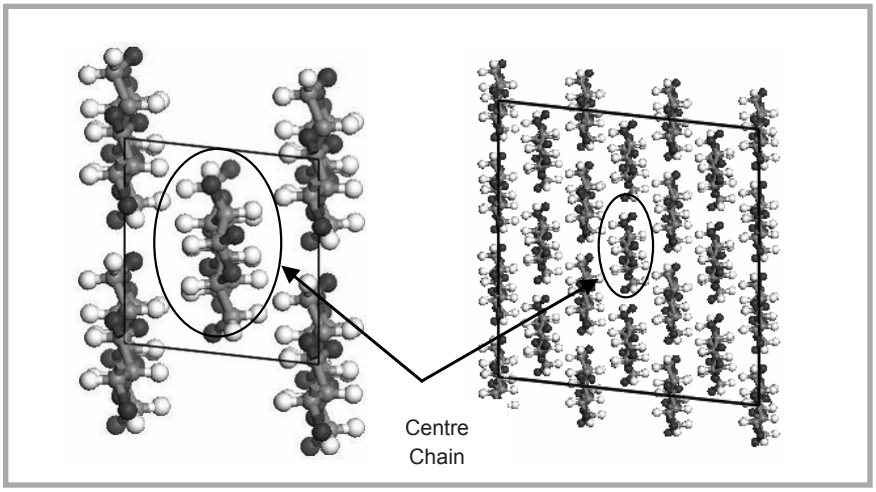

Figure 1. *Structures of cellulose Iβ and the supercell at 300 K.*

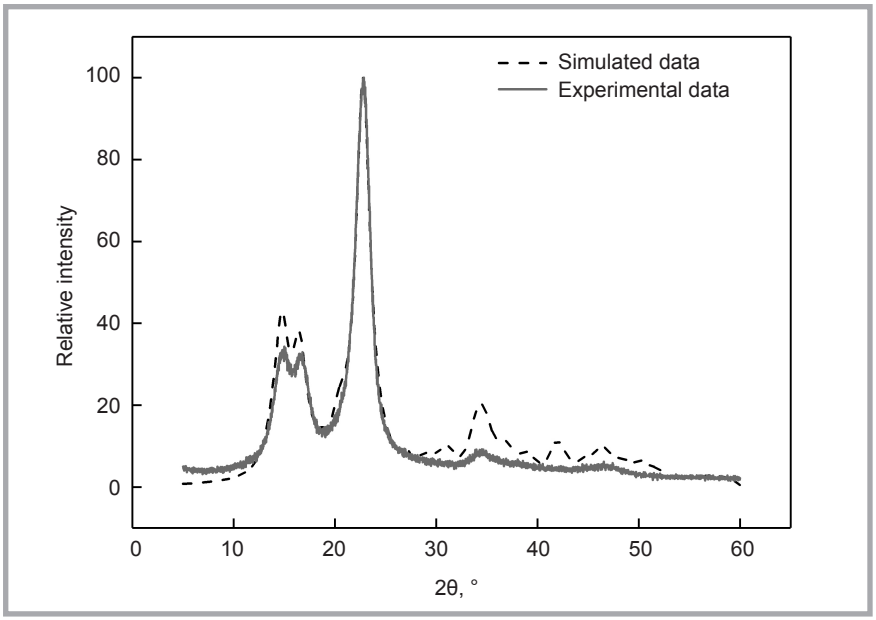

Figure 2. *Simulated and experimental XRD.*

Table 1. *Simulated and experimental results.*

	Simulated results	Experimental results
Crystallinity index, %	75.54%	75.31%
ACS, Å	50	49.51

Where α is the thermal expansion coefficient, and *l* is the unit length in the *a* or *b* direction.

Lattice parameters *a* and *b* with the change of temperature are shown in ***Figure 3***, as reported by Wada [17]. The value of the coefficient of thermal expansion, shown in ***Table 2***, shows that the error between the simulated data and experimental data is not more than 9%. Therefore, it can be considered that the selection of the force field is appropriate and that of the step length reasonable.

Results and discussion

Mulliken population of bonds

The Mulliken population of bonds is an important parameter to describe the strength of chemical bonds [18]. Positive values mean that covalent bonds have been formed between atoms. The greater the positive values are, the stronger the energy of covalent bonds is, and the more stable the bonds between atoms are.

The Mulliken population of cellobiose (the repeat unit) is calculated using the

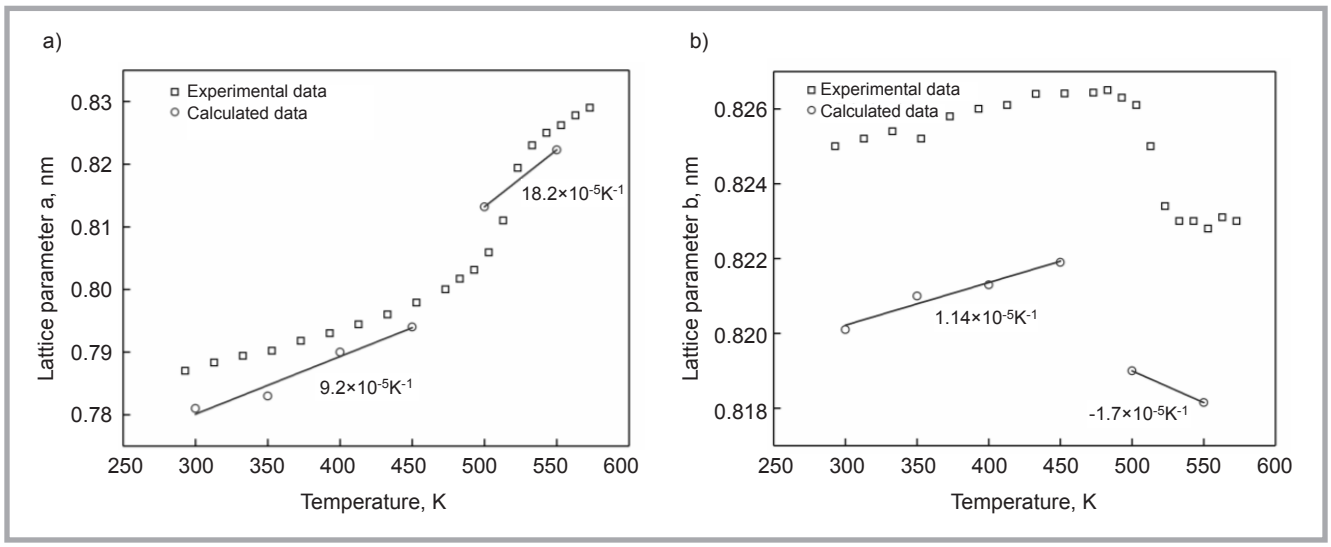

Figure 3. *Variation of lattice parameters a and b: a) Latice parameters a, b) Lattice parameters b.*

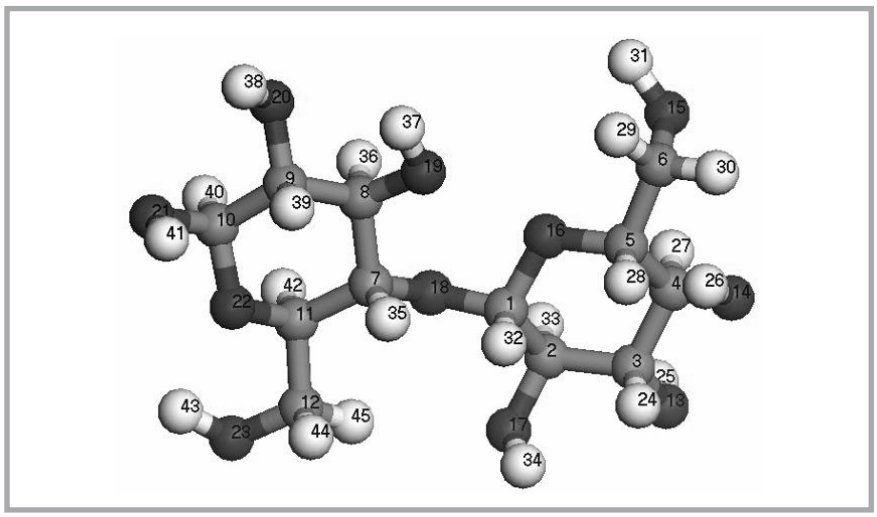

Figure 4. *Structure of cellobiose.*

Table 2. *Values of the thermal expansion coefficient.*

Temperature, K	Thermal expansion coefficient in *a* direction ($10^{-5}\cdot K^{-1}$)			Thermal expansion coefficient in *b* direction ($10^{-5}\cdot K^{-1}$)		
	Calculated data	Experimental data [17]	Error	Calculated data	Experimental data [17]	Error
300 K ~ 450 K	9.2	9.8	6.12%	1.14	1.2	6%
450 K ~ 550 K	18.2	19.8	8.08%	-1.7	-1.6	6.25%

Table 3. *Milliken population of bonds.*

Bond	Bond length, Å	Mulliken population	Bond	Bond length, Å	Mulliken population
C(1)-C(2)	1.541	0.70	C(1)-O(18)	1.414	0.46
C(2)-C(3)	1.529	0.71	C(7)-O(18)	1.455	0.46
C(3)-C(4)	1.528	0.74	C(3)-O(13)	1.446	0.53
C(4)-C(5)	1.532	0.72	C(4)-O(14)	1.418	0.55
C(5)-C(6)	1.525	0.71	C(6)-O(15)	1.445	0.39
C(7)-C(8)	1.554	0.73	C(12)-O(23)	1.452	0.35
C(8)-C(9)	1.553	0.70	C(11)-O(22)	1.450	0.51
C(9)-C(10)	1.557	0.70	C(10)-O(22)	1.437	0.53
C(11)-C(12)	1.535	0.70	C(10)-O(21)	1.401	0.58
C(11)-C(7)	1.550	0.71	C(9)-O(20)	1.435	0.52
C(2)-O(17)	1.457	0.53	C(8)-O(19)	1.432	0.54

CASTEP/geometry optimisation module. The value of Max SCF (self-consistent field) cycles is set to 500, and thr SCF tolerance is 2.0e-4 ev/atom) using the GGA/PW91 basis set.

The value of C-H and H-O bonds' Mulliken population is about 0.85. The Mulliken population of C-C and C-O bonds is shown in ***Table 3***, and the labels of atoms are displayed in ***Figure 4***, where the grey atom is C, the red atom O, and the white atom H.

In ***Table 3***, the values of C-O bonds' Mulliken population are the smallest, followed by C-C bonds, which means that with increasing temperature, C-H bonds and H-O bonds are under the most stable state, followed by C-C bonds, with C-O bonds being under the most unstable state. Among C-O bonds, the Mulliken population values of C-O bonds connecting hydroxyl groups are the smallest, followed by C-O bonds forming glycosidic bonds, and then C-O bonds in a pyranoid ring. According to the values of the Mulliken population, the process of pyrolysis can be divided into three steps: (1) C-O bonds connecting hydroxyl groups begin to break, indicating that part of the glucosyl groups has begun to dehydrate; (2) Cleavage of C-O bonds forming glycosidic bonds occurs, showing the decomposition of glycosidic bonds, resulting in a lower degree of polymerisation; (3) C-O bonds in the pyranoid ring appear to break. Finally, the structure of the cellulose is completely destroyed.

Movement of centre chain

The movement of the chain has a great influence on the thermal stability of cel-

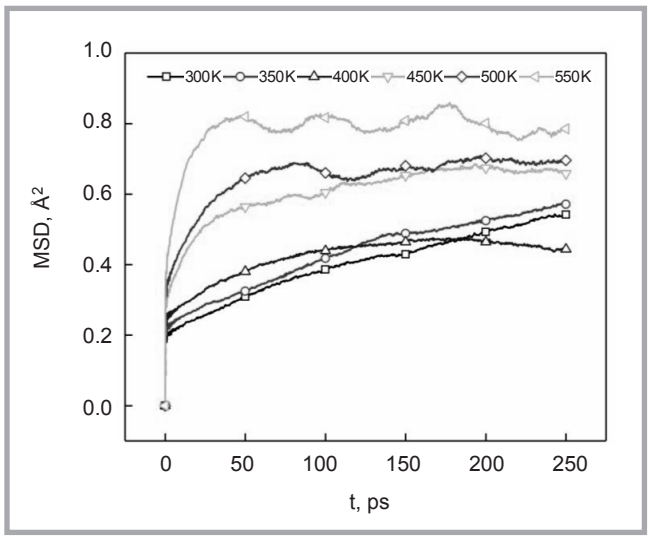

Figure 5. *MSD of the centre chain at different temperatures.*

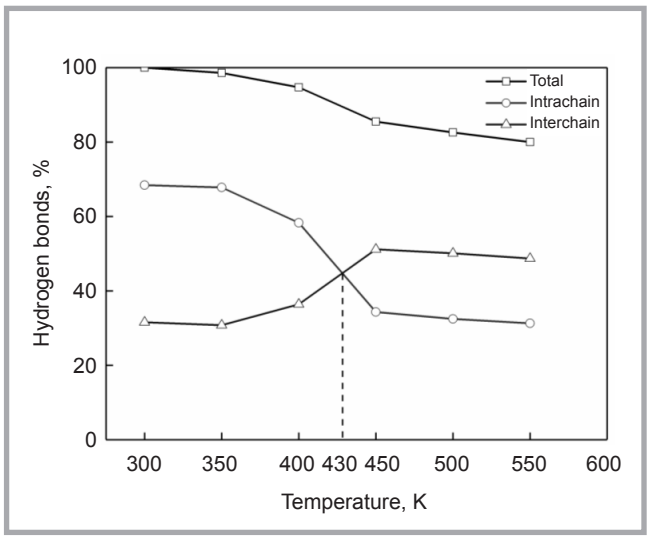

Figure 6. *Changes in hydrogen bonds, plotted as a percentage of the total hydrogen bonds present at 300 K.*

lulose Iβ. The more intense the movement of chains is, the less stable the mechanical properties of cellulose are. MSD (mean square displacement) can be used to characterise the motion of the polymer chain. The detailed meaning of MSD is the average distance of all atoms at moment T. MSD is calculated by ***Equation (4)***:

$$MSD = \left\langle \left| \vec{r_i}(t) - \vec{r_0}(t) \right|^2 \right\rangle \qquad (4)$$

Where $\vec{r_i}(t)$ and $\vec{r_0}(t)$ are the displacement vectors of atom i at moment t and the zero moment, respectively.

250 ps runs were carried out in the NPT ensemble, whose trajectories were used for analysis. During this process, the initial velocity of each molecule was sampled by the Maxwell method, and the Andersen thermal method [19] was used to control the temperature, The Berendsen method [20] was used to control the pressure, the Ewald summation method [21] to calculate the electrostatic potential under periodic boundary conditions, and the atom-based method was used to calculate the Van der Waals (vdW) force. The time step for production runs was 1fs; nonbond interactions were cut off at 9.5 Å; the width of the spline was 1 Å, and that of the buffer 0.5 Å. The target temperature ranged from 300 K to 550 K at intervals of 50 K.

MSD curves of the centre chain (shown in ***Figure 1***) at different temperatures are shown in ***Figure 5***. With increasing temperature, the MSD of the centre chain becomes larger, but this change is not obvious, not showing a strong dependence on temperature. This can be explained by the fact that from 300 K to 550 K, the interaction between cellulose chains and mechanical properties did not fundamentally change, which was proven by the number of hydrogen bonds above. At 400 K the number of intrachain hydrogen bonds decreases sharply, whereas interchain hydrogen bonds increase substantially. This can lead to an exceptional movement of the centre chain, shown in ***Figure 5***.

Hydrogen bonds

Due to the large number of free hydroxyl groups, hydrogen bonds are formed in the intrachain and interchain of cellulose Iβ. Intrachain hydrogen bonds are responsible for chain conformation stability, while interchain hydrogen bonds are responsible for sheet stability [22]. Therefore, hydrogen bonds have great significance in the research of cellulose Iβ performance.

Hydrogen bonds were calculated by means of the Calculate Hydrogen Bonds tool, data of which were monitored by perl script programming. This calculation conditions were as follows: the distances between hydrogen atoms and the acceptor were less than 2 Å, and the angle of hydrogen atoms, the benefactor and acceptor was greater than 110°.

The number of hydrogen bonds changed with increasing temperature, as shown in ***Figure 6***. As the temperature changed from 300 K to 550 K ,the total number of hydrogen bonds decreased by only 20%. Hence, in the whole simulation process, the structure of cellulose Iβ was in a steady state, and hydrogen bonds were not broken in a large quantity when the temperature changed from 300 K to 550 K. Moreover, the mechanical properties of cellulose were not significantly changed. The number of intrachain hydrogen bonds and interchain hydrogen bonds are also shown in ***Figure 4***. Firstly, at 300K the hydrogen bonding number of the intrachain was larger than that of the interchain. But with increasing temperature, the hydrogen bonding number of the intrachain decreased, whereas the hydrogen bonding number of the interchain increased. Then at 430 K, the number of intrachain hydrogen bonds and interchain hydrogen bonds were equal. From 400 K to 450 K, there was the highest rate of change in the intrachain and interchain hydrogen bonding number. Last, at 450 K the hydrogen bonding number of the intrachain and interchain came to restabilise. Thus, the hydroxyl groups involved in intrachain hydrogen bonds at low temperatures form interchain hydrogen bonds at higher temperatures, reaching a new balance and producing a new structure with more stable sheets. This can explain the reason why the cellulose Iβ in natural fibres is not decomposed under 550 K.

Conclusions

In this paper, molecular dynamics simulations were performed to investigate the impact of temperature on the properties of cellulose Iβ using a PCFF force field. The following properties were computed: the Mulliken population, hydrogen

bonds, and movement of the centre chain. The results show that:

(1) With increasing temperature, C-O bonds connecting hydroxyl groups are easily broken, followed by C-O bonds forming glycosidic bonds. And C-O bonds in the pyranoid ring are relatively stable.
(2) With increasing temperature, the MSD of the centre chain became larger, but this change was not obvious, reflecting heat resistance below 550 K.
(3) There was a rupture of intrachain hydrogen bonds and a formation of interchain hydrogen bonds from 400 K ~ 450 K. And at 430 K the number of intrachain hydrogen bonds is equal to that of interchain hydrogen bonds.

Acknowledgements

The authors gratefully acknowledge the financial support of the National Natural Science Foundation of China (51905331) and the cultivation plan of the young scientific research team in Shanghai University of Engineering Science.

References

1. Agarwal J, Mohanty S, Nayak SK. Influence of Cellulose Nanocrystal/Sisal Fiber on the Mechanical, Thermal, and Morphological Performance of Polypropylene Hybrid Composites [J]. *Polymer Bulletin* 2021; 78(16): 1609-1635.
2. Hayashi N, Kondo T. Enzymatically Produced Nano-Ordered Elements Containing Cellulose Iβ Crystalline Domains of Cladophora Cellulose. *Handbook of Polymer Nanocomposites. Processing, Performance and Application* 2015; 61(2): 1-14.
3. Dri FL, Jr LGH, Moon RJ, et al. Anisotropy of the Elastic Properties of Crystalline Cellulose Iβ from First Principles Density Functional Theory with Van Der Waals Interactions. *Cellulose* 2013; 20(6): 2703-2718.
4. Fan B, Maranas JK. Coarse-Grained Simulation of Cellulose Iβ with Application To Long Fibrils. *Cellulose* 2015, 22(1): 31-44.
5. Okano T, Koyanagi A. Structural Variation of Native Cellulose Related to Its Source. *Biopolymers* 2010; 25(5): 851-861.
6. Chen P, Nishiyama Y, Mazeau K. Atomic Partial Charges And One Lennard-Jones Parameter Crucial To Model Cellulose Allomorphs. *Cellulose* 2014, 21(4): 2207-2217.
7. Wada M, Hori R, Kim, UJ, et al. X-Ray Diffraction Study on the Thermal Expansion Behavior of Cellulose Iβ and Its High-Temperature Phase. *Polymer Degradation and Stability* 2010; 95(8): 1330-1334.
8. Pan C, Yu O, Yoshiharu N, et al. Iα to Iβ Mechano-Conversion and Amorphization in Native Cellulose Simulated by Crystal Bending. *Cellulose* 2018; 25(8): 1-11.
9. Watanabe A, Morita S, Ozaki Y. Temperature-Dependent Structural Changes in Hydrogen Bonds in Microcrystalline Cellulose Studied by Infrared and Near-Infrared Spectroscopy with Perturbation-Correlation Moving-Window Two-Dimensional Correlation Analysis. Applied Spectroscopy 2006; 60(6): 611-618.
10. Bergenstråhle M, Berglund LA, Mazeau K. Thermal Response in Crystalline Iβ Cellulose: a Molecular Dynamics Study. *The Journal of Physical Chemistry B* 2007; 111(30): 9138-9145.
11. Agarwal V, Huber G , Conner WC, et al. Simulating Infrared Spectra and Hydrogen Bonding in Cellulose Iβ at Elevated Temperatures. *The Journal of Chemical Physics* 2011; 135(13): 134-506.
12. Maple JR, Hwang MJ, Stockfisch TP, et al. Derivation of Class II Force Fields. I: Methodology and Quantum Force Field for the Alkyl Functional Group and Alkane Molecules. *Journal of Computational Chemistry* 2010; 15(2): 162-182.
13. Maple JR, Hwang MJ, Stockfisch TP, et al. Derivation of Class II Force Fields. III. Characterization of a Quantum Force Field for Alkanes. *Israel Journal of Chemistry* 2013; 34(2): 195-231.
14. Nishiyama Y, Langan P, Chanzy H. Crystal Structure and Hydrogen-Bonding System in Cellulose Iβ from Synchrotron X-Ray and Neutron Fiber Diffraction. *Journal of the American Chemical Society* 2002; 124(31): 9074-9082.
15. Wang Y, Zhao Y, Deng Y. Effect of Enzymatic Treatment on Cotton Fiber Dissolution in Naoh/Urea Solution at Cold Temperature. *Carbohydrate Polymers* 2008; 72(1): 178-184.
16. Birks L, Friedman H. Particle Size Determination from X-Ray Line Broadening. *Journal of Applied Physics* 1946; 17(8): 687-692.
17. Wada M, Hori R, Kim UJ, et al. X-Ray Diffraction Study on the Thermal Expansion Behavior of Cellulose Iβ and Its High-Temperature Phase. *Polymer Degradation & Stability* 2010; 95(8): 1330-1334.
18. Li YF, Xiao B, Sun L, et al. Phonon Optics, Thermal Expansion Tensor, Thermodynamic and Chemical Bonding Properties of Al4SiC4 and Al4Si2C5: A First-Principles Study. *Rsc Advances* 2016; 6(49): 43191-43204.
19. Andrea TA, Swope WC, Andersen HC. The Role Of Long Ranged Forces In Determining The Structure And Properties Of Liquid Water. *Journal of Chemical Physics* 1983; 79(9): 4576-4584.
20. Berendsen HJC, Postma JPM, Gunsteren WFV, et al. Molecular Dynamics with Coupling to an External Bath. *Journal of Chemical Physics* 1984; 81(8): 3684-3690.
21. Ewald PP. Ewald Summation [J]. Annalen der Physik, 1921, 369(3): 253-287.
22. Jarvis M. Chemistry: cellulose stacks up. *Nature* 2003, 426(6967): 611-612.

Received 12.06.2018 Reviewed 23.06.2021